EUKARYOTIC CELL, Feb. 2007, p. 157–170 Vol. 6, No. 2
1535-9778/07/$08.00+0 doi:10.1128/EC.00247-06

High Viscosity and Anisotropy Characterize the Cytoplasm of Fungal Dormant Stress-Resistant Spores▽

J. Dijksterhuis,[1,2]* J. Nijsse,[3]† F. A. Hoekstra,[3] and E. A. Golovina[3]

Applied and Industrial Mycology, CBS Fungal Biodiversity Centre, Uppsalalaan 8, 3584 CT, Utrecht,[1] Agrotechnology and Food Innovations and Wageningen Centre for Food Sciences (WCFS), P.O. Box 557, 6700 AN Wageningen,[2] and Laboratory of Plant Physiology, Wageningen University, Arboretumlaan 4, 6703 BD Wageningen,[3] The Netherlands

Received 1 August 2006/Accepted 31 October 2006

Ascospores of the fungus *Talaromyces macrosporus* are dormant and extremely stress resistant, whereas fungal conidia—the main airborne vehicles of distribution—are not. Here, physical parameters of the cytoplasm of these types of spores were compared. Cytoplasmic viscosity and level of anisotropy as judged by spin probe studies (electron spin resonance) were extremely high in dormant ascospores and during early germination and decreased only partly after trehalose degradation and glucose efflux. Upon prosilition (ejection of the spore), these parameters fell sharply to values characteristic of vegetative cells. These changes occurred without major volume changes that suggest dramatic changes in cytoplasmic organization. Azide reversibly inhibited prosilition as well as the decline in cytoplasmic parameters. No organelle structures were observed in etched, cryoplaned specimens of ascospores by low-temperature scanning electron microscopy (LTSEM), confirming the high cytoplasmic viscosity. However, cell structures became visible upon prosilition, indicating reduced viscosity. The viscosity of fresh conidia of different *Penicillium* species was lower, namely, 3.5 to 4.8 cP, than that of ascospores, near 15 cP. In addition the level of anisotropic motion was markedly lower in these cells ($h_0/h_{+1} = 1.16$ versus 1.4). This was confirmed by LTSEM images showing cell structures. The decline of cytoplasmic viscosity in conidia during germination was linked with a gradual increase in cell volume. These data show that mechanisms of cytoplasm conservation during germination differ markedly between ascospores and conidia.

Ascospores of the fungus *Talaromyces macrosporus* are sexual structures that exhibit extreme resistance to heat, high pressure, drought, and freezing (14, 15). They contain an extremely high level of trehalose (13) and have relatively low amounts of water in an aqueous environment. The spores show constitutive dormancy in rich media, and germination is triggered and synchronized by a short heat treatment at 85°C. Ascospores of *T. macrosporus* can germinate after 17 years of storage (40) and belong to the most resilient eucaryotic structures described hitherto. They can survive a heat treatment at 85°C for 100 min or high pressurization at 1,000 MPa for 5 min (14). Upon heat activation, the spores degrade their trehalose within 100 min, followed by a rapid release of glucose into the bathing medium up to 10% of the cell wet weight. After 2.5 h, the outer cell wall opens, and the protoplast encompassed by the inner cell wall is ejected in a fast process (seconds) termed prosilition. The ejected cell then swells and forms a germ tube, resembling events that occur in other fungal spores. Conner et al. (10) studied the cellular basis of heat resistance in relatively young (11-day) and older (25-day) ascospores of *Neosartorya fischeri* exhibiting different heat resistance levels (D_{82} of approximately 23 and >60 min, respectively). The ascospores showed differences in the inner cell wall region at the lateral ridge of the spore and also qualitative differences in extractable proteins but did not differ in fatty acid or lipid content. The old spores contained higher levels of mannitol and trehalose than the young ones did. The relatively low water content and high level of trehalose in ascospores of *T. macrosporus* might create a high viscosity in the spore cytoplasm and thus provide the physical conditions for low metabolism, which relate to dormancy and high stress tolerance.

Conidia are fungal spores that are distributed through the air, where they are dominant fungal vehicles for distribution. Conidia are cells that have lower heat resistance (see for instance the work of Scholte et al. [49]) than the ascospores of *T. macrosporus* and exhibit no constitutive dormancy (according to references 6 and 51). Conidia of *Aspergillus niger* and *Aspergillus nidulans* contain lower levels of trehalose and mannitol inside the cytoplasm than the ascospores of *T. macrosporus*. These compatible solutes are thought to function in protection against heat. Trehalose has been found to be important for survival during prolonged storage of conidia (18, 47).

It is an axiom that biochemical processes are dependent on the properties of the medium, which, in the case of living cells, is the cytoplasm. The aqueous cytoplasm of cells is a complex non-Newtonian fluid consisting of a lattice of filamentous elements and associated macromolecules (32) and dissolved small proteins and macrosolutes. The fluid-phase cytoplasmic viscosity (or microviscosity) is defined as the viscosity sensed by small, noninteracting probe molecules. Fluid-phase cytoplasmic viscosity is thought to be very important in relation to the diffusion of metabolites and diffusion-limited enzyme kinetics (3, 12). In addition, high viscosity can inhibit protein unfolding

* Corresponding author. Mailing address: Department of Applied and Industrial Mycology, Centraalbureau voor Schimmelcultures, Uppsalalaan 8, 3584 CT Utrecht, The Netherlands. Phone: 31.30.2122654. Fax: 31.30.2512097. E-mail: Dijksterhuis@cbs.knaw.nl.

† Present address: Unilever R&D, P.O. Box 114, 3130 AC Vlaardingen, The Netherlands.

▽ Published ahead of print on 10 November 2006.

(11, 23, 27). High viscosity might protect against heat stress by counteracting the effect of elevated temperature on diffusion in the cytoplasm and protein unfolding.

In living cells, the fluid-phase viscosity (or microviscosity) has been estimated by different techniques that quantify the mobility of small tracer particles. One of the approaches providing realistic values of cytoplasmic viscosity is based on fluorescent probes (16, 31). Although the range of values obtained is quite broad, thorough analysis of the available data indicates that the fluid-phase cytoplasmic viscosity does not exceed 3 to 4 cP (32). Later, separation of the signals from bound and nonbound fluorescent probes by time-resolved analysis of the fluorescence decay has allowed for more precise information on cytoplasmic viscosity (20). Thus, the fluid-phase viscosity in Swiss 3T3 fibroblasts was not much higher than that in water (1.2 to 1.4 cP), and these low values of cytoplasmic viscosity have been confirmed by others (33, 44). Slightly higher values have been found for sea urchin eggs (2.1 to 2.5 cP [43]) and plant cells (1.1 to 3.7 cP [50]).

Spin label electron spin resonance (ESR) spectroscopy is another promising approach to measure cytoplasmic viscosity (25). Thus, estimates of cytoplasmic viscosity mainly range from 2 to 4 cP for mammalian and plant cells (29, 35, 37, 39, 48), values which are comparable with those obtained with fluorescent probes (17, 30, 31). The spin probe TEMPONE (4-oxo-2,2,6,6-tetramethylpiperidine-*N*-oxy) is particularly suitable to study rotational mobility in the cytoplasm, because the molecule is small and water soluble, easily penetrates the cell, and resides mainly in the aqueous fluid phase.

In this paper we present data on the viscosity of the cytoplasmic fluid phase in ascospores of *T. macrosporus* and conidia of related *Penicillium* species at different stages of germination, from dormancy to prosilition/germination. The data on viscosity were derived from the ESR spectra of perdeuterated TEMPONE (PDT) in cytoplasm and supported by micrographs obtained by low-temperature scanning electron microscopy (LTSEM) of cryoplaned samples. Very high effective cytoplasmic viscosity and a very high level of anisotropic motion were found for dormant *T. macrosporus* ascospores. Also, the time lag between dormancy and prosilition was characterized by high values, but a dramatic and fast decrease in the values of these two parameters was noticed with prosilition. By comparison, conidia of different *Penicillium* species had much lower cytoplasmic viscosity and anisotropy that gradually decreased with time of germination. The data suggest that the steep decrease in cytoplasmic microviscosity of ascospores without volume increase, which corresponds with the return to vegetative growth, includes sudden changes in the structural organization of the cytoplasm, while the slow decrease in microviscosity of conidia is linked only with the gradual increase in cytoplasmic volume.

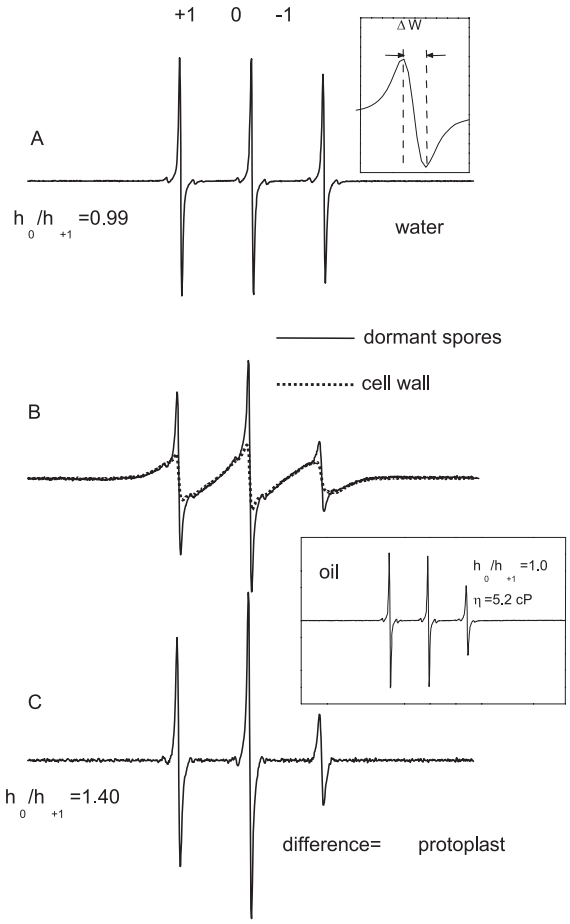

FIG. 1. ESR spectra of dormant ascospores. (A and B) ESR spectra of PDT in water (A) and in dormant *T. macrosporus* ascospores (B). The dotted line in panel B is the PDT spectrum from cell walls of dormant spores. (C) The result of the subtraction of the cell wall spectrum from the total spectrum from dormant ascospores, representing the spectrum of PDT in the aqueous fluid phase of the spore protoplast. This spectrum is used to calculate cytoplasmic viscosity. The line heights of the low-field, central, and high-field lines are designated h_{+1}, h_0, and h_{-1}, respectively. The degree of anisotropy is indicated by h_0/h_{+1}. The inset in panel C is the spectrum of PDT in plant oil. This spectrum shows isotropic rotation of spin label molecules in the homogeneous environment of high viscosity.

MATERIALS AND METHODS

Organism, growth conditions, and harvesting of spores. *Talaromyces macrosporus* CBS 130.89 Stolk and Samson (19) was grown on oatmeal agar surfaces at 30°C. Ascospores were harvested as described before (13). For the different experiments fungal cultures were used that were 5 to 8 weeks old and had acquired heat resistance and constitutive dormancy (14). Conidia of *Penicillium roqueforti* CBS 135.67 and *Penicillium crustosum* CBS 101025 were harvested after 7 to 10 days of growth on malt extract agar at 24°C. In addition, a strain of *Penicillium discolor*, CBS 611.92, was used that had evolved a natural mutant with white conidia, and both conidia of the green strain and those of the white strain were harvested after 7 days of growth on malt extract agar and used for ESR experiments.

ESR experiments. Ascospore suspensions with a density of approximately 10^8 spores/ml were used. The spores were activated for 7 min at 85°C in a small Erlenmeyer flask and then incubated in a water bath at 100 to 150 strokes/min. For cultivation ACES [*N*-(2-acetamido)-2-aminoethanesulfonic acid] buffer supplemented with 0.05% Tween 80 was used (13). The nitroxide spin probe PDT (provided by I. Grigoriev, Institute of Organic Chemistry of the Russian Academy of Sciences, Novosibirsk, Russia) was utilized for labeling the spores. Potassium ferricyanide was added to the PDT solution to broaden the signal of PDT outside the spores. The final concentrations of PDT and potassium ferricyanide in the bathing solution were 1 mM and 120 mM, respectively. Because ferricyanide ions do not penetrate membranes while TEMPONE (or PDT) molecules can (21), the ESR signal of PDT located inside the cell cannot be broadened and can thus be separated from the broadened signal originating from outside the spores. The narrow lines of the nonbroadened signal of PDT can be used to calculate cytoplasmic viscosity and level of anisotropic motion.

Samples were taken at regular time intervals during germination, from 0 to 280 min after the start of heat activation; ascospores were spun down in an Eppen-

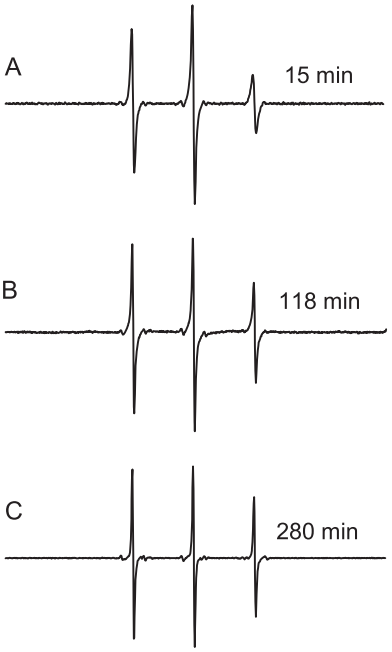

FIG. 2. Changes in ESR spectra during germination of ascospores. Shown are the narrow components of ESR spectra of PDT in ascospores of *T. macrosporus* 15, 118, and 280 min after the start of heat activation.

dorf cup, resuspended in the TEMPONE-ferricyanide mixture for labeling, and then transferred with a microsyringe to a 2-mm-diameter capillary. After a few minutes of labeling, the capillary was centrifuged again, the excess of supernatant was removed, and the capillary was placed in an ESR tube for spectrum recording. ESR spectra were recorded with an X-band ESR spectrometer (model 300E; Bruker Analytik, Rheinstetten, Germany). To prevent overmodulation and saturation of the ESR signal, the microwave power was limited to 2 to 5 mW and the modulation amplitude was 0.25 G. Field scan widths of 100 G were used to record the entire spectrum. In addition, spectra were acquired from ascospores in the presence of sodium azide. Spores were heat activated as described above, and directly after the heat treatment azide was added to a final concentration of 5 mM.

Control spectra were acquired for a fraction of broken cell walls of dormant and activated ascospores without cytoplasm. For this, ascospores were vortexed in the presence of 1-mm-diameter glass beads till the majority of the cells were broken. The suspension was removed from the glass beads with a pipette and washed in buffer.

Conidia of *P. roqueforti*, *P. crustosum*, and *P. discolor* were added to malt extract broth and incubated at 25°C in an Erlenmeyer flask at a density of approximately 10^8 cells/ml and treated similarly to ascospores during ESR measurements. Green and white conidia of *P. discolor* were incubated at 28°C in malt extract broth. Conidia of the *Penicillium* species displayed an endogenous ESR signal from nonlabeled (green) spores that contained melanins. The g value was determined by direct comparison of the position of the signal (singlet) with the position of the signals (singlets) from two standard compounds with known g factors inserted besides the specimen. One standard was the crystal of diphenylpicrylhydrazyl with a g value of 2.0036, and another standard was Bruker strong pitch with a g value of 2.0028. The g value of the sample can be calculated according to the formula $g(sp) = g(st)[1 - (B_{st} - B_{sp})/B_{sp}]$, where B_{st} is the position (field strength) of the standard and B_{sp} is the position of the signal of the sample.

Calculation of cytoplasmic microviscosity and anisotropy from ESR spectra. Quantitatively, molecular rotation is characterized by the rotational correlation time τ_R. According to the Stokes-Einstein-Debye theory of liquid state, correlation times depend on the size of the molecule and the bulk viscosity of the solvent. If the PDT molecule is approximated by a rigid sphere with a radius of 3 Å rotating in a medium of viscosity η, then the isotropic rotational correlation time $\tau_R = 4\pi(3)^3\eta/3kT$ (Stokes-Einstein relationship), where k is the Bolzmann constant and T is the absolute temperature in kelvins. The rotational correlation time of the spin probe can be used to calculate the microviscosity of the medium according to the above formula if the size of the probe is larger than that of the solvent molecule.

The rotational correlation time can be derived from the shape of the ESR spectra. The spectra of 1 mM PDT in water have three narrow equidistant lines (Fig. 1A). These lines are particularly narrow because replacement of protons by deuterons eliminates line broadening due to nonresolved hyperfine interaction of

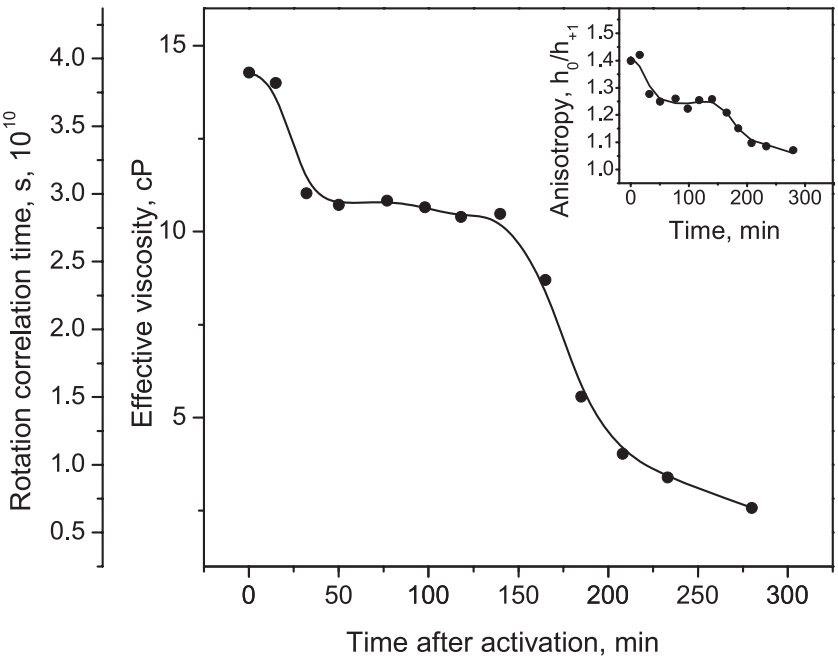

FIG. 3. Changes in rotational correlation time and effective viscosity of the cytoplasm of germinating *T. macrosporus* ascospores with time after the start of heat activation. Calculation of viscosity is based on rotational correlation times derived from the shape of the ESR spectra of PDT in the cytoplasm. The inset shows the parameter of anisotropic motion.

^{14}N with protons. To calculate rotational correlation times from ESR spectra, we used the simplified equation proposed by Keith and Snipes (24). This equation is valid for isotropic fast Brownian motion ($\tau < 10^{-9}$ s): $\tau_R = 6.5\ 10^{-10}\ \Delta W_0$ ($\sqrt{h_0/h_{-1} - 1}$), where ΔW_0 is the peak-to-peak width of the central line (Fig. 1A, inset) and h_0 and h_{-1} are the line heights of the central and high-field lines, respectively. However, in vivo, spin labels may undergo anisotropic motion because of the submicroscopic intermolecular organization (32). In such a case rotational correlation times calculated from the shape of the spectra might be not real but present some relative index of rotation, which includes not only rotation in water solution but different types of interactions in the crowded cytoplasm. Calculated viscosity is therefore not true viscosity but "apparent" or "effective" viscosity that reflects the physical properties of the cytoplasm, including both viscosity of the fluid phase and contribution of the structural organization. Henceforth, we will use the term "viscosity" as the integral physical characteristic of the cytoplasmic environment. To characterize anisotropic rotation of spin probes in the cytoplasm (preferential rotation of the molecule about one of the molecular axes), we used the parameter h_0/h_{+1}, where h_0 and h_{+1} are the line heights of the central and low-field lines, respectively (26).

Cryoplaning. Samples were taken for cryofixation from dormant ascospores and from spores at intervals after the beginning of heat activation. In addition, freshly harvested conidia of *Penicillium roqueforti* and *P. crustosum* were prepared for cryoplaning. The spores were quickly spun down in an Eppendorf centrifuge, and a droplet of the pellet was placed on top of small rivets (4-mm-long aluminum pins with a head) and immediately plunge-frozen in liquid propane. These rivets fitted into sample holders for cryoplaning and SEM investigation of the specimens. For cryoplaning (reviewed in reference 42), the frozen droplets were sectioned with a glass knife in a cryoultramicrotome (Reichert-Jung Ultracut E/FC4D; Vienna, Austria) to examine the contents of the spores. The last sections were cut using a diamond knife at decreasing section thicknesses from 0.5 μm to 20 nm and at decreasing sectioning speeds down to 0.2 mm s^{-1}. During planing, the sample temperature was −90°C and the knife temperature was −100°C. The samples were stored in liquid nitrogen and cryotransferred to a low-temperature scanning electron microscope (JEOL 6300F field emission SEM; Tokyo, Japan). The planed samples were freeze-etched for 3 min at −89°C to enhance contrast and remove water vapor contamination, sputter coated with platinum, and subsequently analyzed at −190°C with an accelerating voltage of 5 kV.

Physiological parameters. Respiration and sugar content of ascospores were measured as described by Dijksterhuis et al. (13). For trehalose analysis, the suspension was split into two aliquots of 5 ml and heat activated. To one of them, sodium azide was added to a final concentration of 5 mM, and at regular time intervals samples were taken. At 198 to 210 min after the beginning of the experiment (including heat activation) the azide was removed by washing the cells twice with 40 ml ACES buffer (2,500 rpm, 5 min). Cells were resuspended at the same density and incubated under the same conditions. Supernatant was collected (after very brief centrifugation) for the detection of sugars released by the spores, and the cells were resuspended in buffer and broken as described earlier (13) for the detection of intracellular sugars. The optical density and oxygen consumption of spore suspensions were measured according to the method of Dijksterhuis et al. (13).

Measurement of spore size. Conidia of *P. crustosum* and *P. roqueforti* were inoculated on malt extract broth at 24°C, and the flasks were agitated at 120 rpm. Ascospores of *T. macrosporus* were harvested as described before (13), heat activated, and subsequently inoculated in malt extract broth at 30°C and 120 rpm. Spores were visually inspected at time intervals during incubation by a light microscope (Zeiss Axioplan; Oberkochen, Germany) equipped with a 100× objective by using the phase-contrast mode. Micrographs were analyzed in Adobe Photoshop. Spore boundaries were selected with the magic wand tool, and cell size was expressed as pixel number. At least 25 spores per developmental stage were analyzed.

RESULTS

ESR spectra reveal a very high viscosity and anisotropy in dormant ascospores, which decrease during germination. The ESR spectrum of PDT in dormant ascospores contained two components, narrow and broad (Fig. 1B). The broad component had the same shape as the PDT spectrum from isolated cell wall in broadened solution of PDT. Subtraction of the broad component gave the shape of the narrow component (Fig. 1C). The distance between the equidistant lines, which is measured between the points where the spectrum crosses the baseline, was 15.9 to 16.0 G, close to that in the spectrum of PDT in water (16.1 G, Fig. 1A). This distance, the so-called isotropic hyperfine splitting constant, a_{iso}, is indicative of the polarity of the environment. The narrow component in the ascospore spectrum therefore represents PDT molecules in an environment with a polarity close to that in water. The narrow character of this component also means that the compartment where the PDT molecules reside is not accessible to ferricyanide ions from the medium. Together, these characteristics allow for the assignment of the narrow component of the spectrum in Fig. 1B to PDT molecules in the aqueous phase of the spore cytoplasm. Further, we will deal only with the narrow component of PDT spectra. The broad character of the ferricyanide-broadened PDT spectrum from isolated spore walls (Fig. 1B) is typical for porous materials.

Although the PDT spectra in Fig. 1A and C both have narrow lines and similar a_{iso}, the spectra from water and from the fluid phase of the spore cytoplasm have different propor-

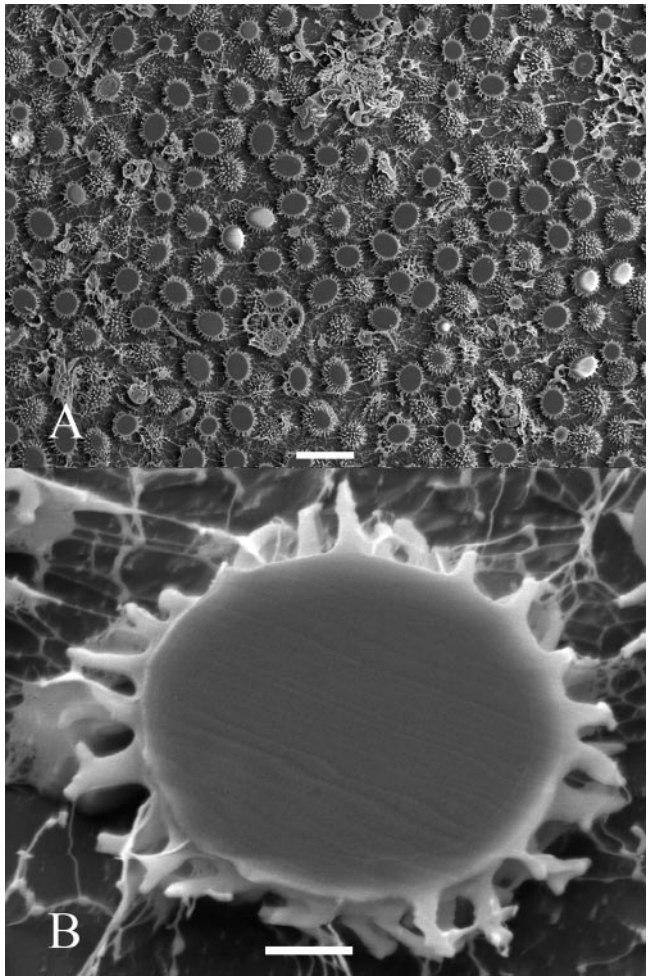

FIG. 4. LTSEM micrographs of etched, cryoplaned *T. macrosporus* dormant ascospores. (A) Pelleted spore cells showing polished cell profiles. (B) Detail of one ascospore showing extensive ornamentation on the spore wall but no features of organelles inside the cell. As a result of cutting of the cells and subsequent etching, both the cell surface and the interior are visible. Bar, 10 μm (A) or 1 μm (B).

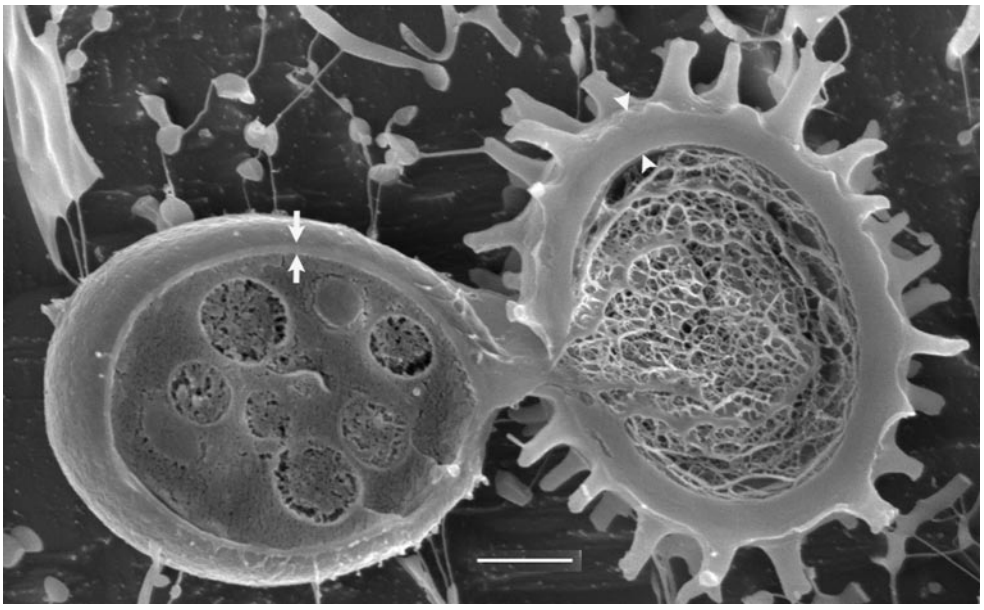

FIG. 5. LTSEM micrographs of an etched, cryoplaned *T. macrosporus* ascospore after prosilition. Note the thick outer cell wall (delineated by arrowheads) and the thin inner cell wall (delineated by arrows) encompassing the protoplast. Inside the cytoplasm, cell organelles can be easily discerned. Bar, 1 μm.

tions between line heights. While the height of the central line (designated 0) was almost equal to that of the low-field line (designated +1) in the spectrum from water (Fig. 1A, ratio of 0.99), the height of the central component in the spectrum from the spore cytoplasm was considerably greater than that of the low-field component (Fig. 1C, ratio of 1.40). The height of the high-field line (designated −1) relative to the central line in the spectrum from the cytoplasm (Fig. 1C) was considerably lower than that in the spectrum from water (Fig. 1A). This means that PDT molecules in water have almost isotropic rotation in a low-viscosity environment, whereas in the cytoplasm of dormant ascospores the PDT molecules experience anisotropic rotation (h_0/h_{+1}) in a high-viscosity environment (proportional to h_0/h_{-1}; see Materials and Methods). As a comparison, the spectrum of PDT in seed oil is shown in the inset of Fig. 1C. The spectral parameters ($h_0/h_{+1} = 1$; $h_0/h_{-1} = 1.72$; $\eta =$ 5.2 cP) show that the rotation of PDT molecules in oil is slow but isotropic. Further, an ESR spectrum of PDT in 50% polyethylene glycol 6000 (not shown) is characterized by a h_0/h_{+1} value of 1 (isotropic motion as in water) and a viscosity of approximately 2 cP. This is interpreted as a sufficient free volume between the polyethylene glycol macromolecules for the spin label motion to experience no restrictions in spite of high macroviscosity.

Heat activation did not cause immediate changes in the narrow component of the ESR spectra (Fig. 2A). However, the shape of the spectra changed with time after heat activation in that the height difference between the lines became less (compare Fig. 2A with Fig. 2B and C). In terms of spectral parameters this means that with time after heat activation the rotation correlation time of the spore cytoplasm decreased and also the parameter of anisotropic motion decreased. Figure 3 shows the changes in rotational correlation time and related effective viscosity of the ascospore cytoplasm with time after the start of heat activation. It reveals a very high initial viscosity of near 15 cP, which was correlated with a high anisotropy ($h_0/h_{+1} = 1.4$) for dormant ascospores. After heat activation there was a relatively fast but restricted decrease in viscosity from 15 to 10 cP during the first half-hour. Thereafter, there was a period of 100 min in which the cytoplasmic viscosity did not change. The second, major decrease in viscosity occurred at 150 min after the start of heat activation and correlated with spore prosilition. The same changes occurred in the level of anisotropic motion (Fig. 3, inset).

Cryoplaning studies confirm a major change in the cytoplasmic organization after prosilition. In addition to ESR studies, the interior of the ascospores was observed with LTSEM. An overview of a cryoplaned pellet of dormant spores is shown in Fig. 4A, where numerous cut spores can be seen. During etching, the ice between the spores was sublimed away, which revealed the ornamentation of the outer cell wall. Figure 4B shows a detail, illustrating that intracellular features can hardly be discerned in dormant spores. This could be expected when highly viscous cytoplasm becomes an amorphous, glassy mass upon being plunged in liquid propane. The glassy state does not allow water to be sublimed during etching. However, prosilition led to considerable changes in the appearance of the cryoplaned cells (Fig. 5). The protoplast encompassed by a relatively thin cell wall (arrow) was ejected through a thick, ornamented outer cell wall, which appeared to be ruptured (Fig. 6, top). Also, a third layer of the cell wall became apparent, which is characterized by its fibrillose nature after etching (Fig. 5 and 6, top). Strands of material from this layer ran from the inside of the emptied cell wall over the surface of the expelled cell and formed a connection between these two entities (Fig. 6, middle and bottom). Indeed, expelled cells were connected to the emptied cell walls for a prolonged time during fungal development. Figure 5 also shows that organelles

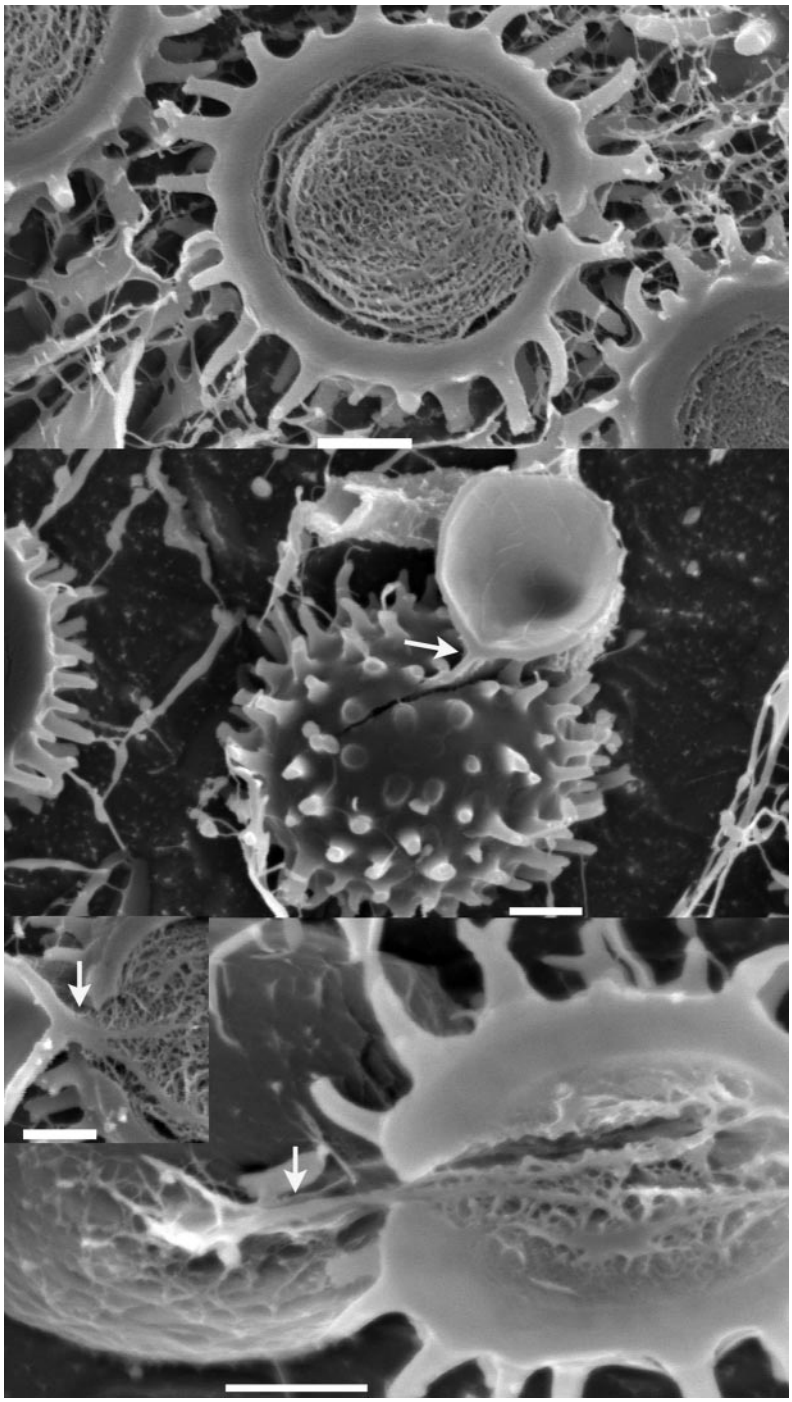

FIG. 6. LTSEM micrographic details of etched, cryoplaned *T. macrosporus* ascospores after prosilition. The ejected cell is connected with the outer cell wall by a third layer of cell wall material that appears fibrillar under these conditions. (Top) Rupture of the thick outer cell wall after prosilition at the right side of the cell. (Middle) The rupture of the thick outer wall runs along the ellipsoidal spore, which is visible when the ejected cell is removed almost completely by cryoplaning. However, this cell remains connected with the cell wall (arrow). (Bottom) Here, the outer cell layer is almost removed, which confirms the connection between the ejected cell and the cell wall (arrow). The inset shows a detail of another cell where the connecting material is continuous with the fibrillar material. Bars, 1 μm.

inside the expelled cells are readily visible, apparently because no glass was formed upon the plunging of the cells in liquid propane. These cells had an internal viscosity of around 2 cP (Fig. 3), which is typical of vegetative cells. The emptied cells did not contain organelles, which indicates that the entire protoplast was ejected through the slit in the ornamented outer wall. Figure 7 summarizes different stages of germination of ascospores as viewed after cryoplaning and correlated with the fluid-phase viscosity. Prosilition is correlated with a strong decrease in viscosity (ESR), and the visibility

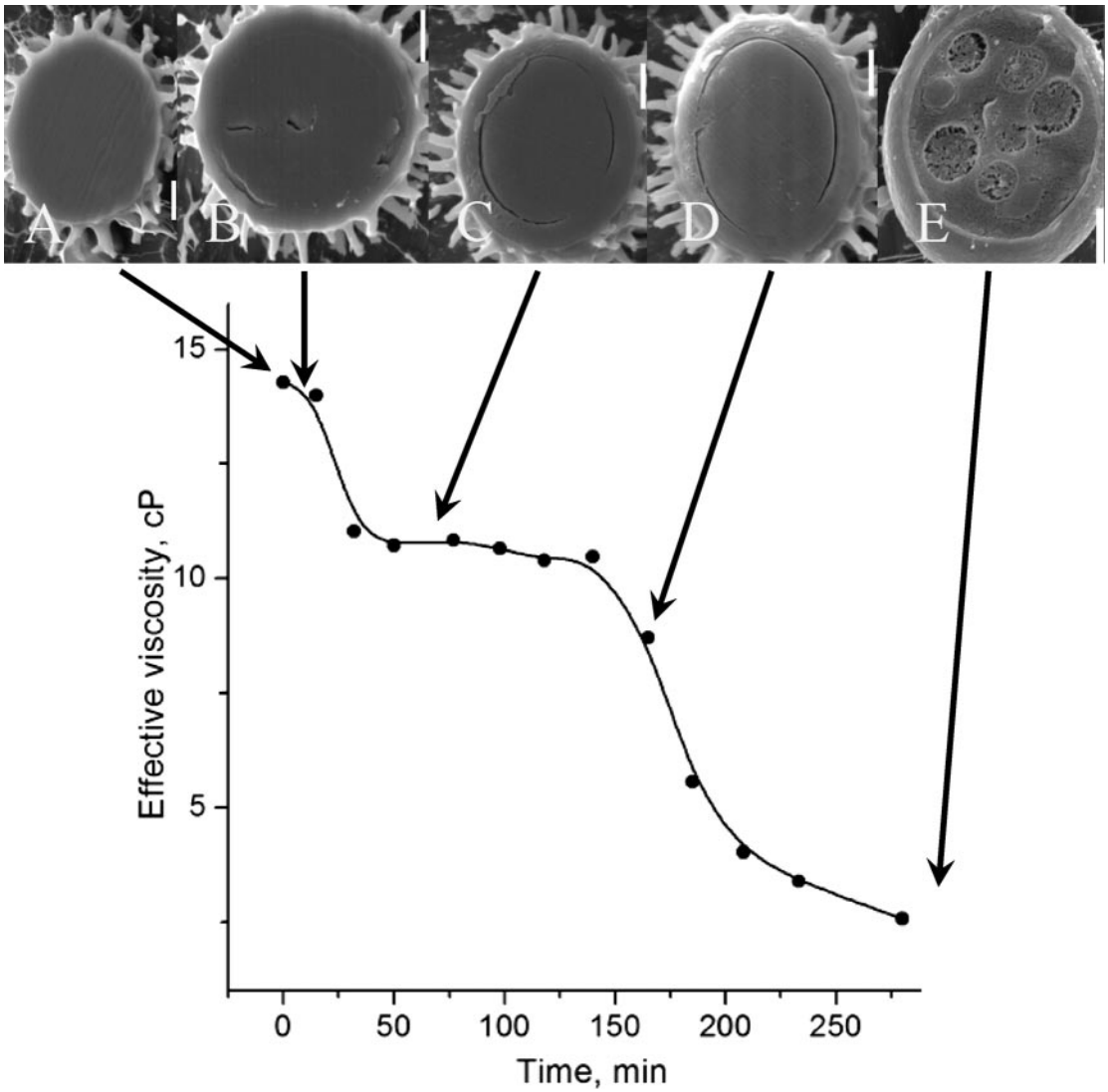

FIG. 7. Comparison of LTSEM pictures and viscosity during germination of ascospores. Shown are LTSEM micrographs of etched, cryoplaned *T. macrosporus* ascospores at different stages of early germination (0 [A], 16 [B], 75 [C], 177 [D], and 300 [E] min after activation) compared with the viscosity data of Fig. 3. In panel D, faint outlines of organelles can be observed, while organelles are clearly visible in panel E. Bars, 1 μm.

of cell structures is correlated with reduced viscosity. In Fig. 7D, cell organelles became faintly visible, while they were clearly visible in Fig. 7E.

Inhibition of prosilition is correlated with prolonged high viscosity and anisotropy. To be able to attribute the changes in cytoplasmic viscosity to specific events during ascospore germination, the respiration inhibitor azide was applied directly after heat activation. In the presence of azide, spore prosilition was blocked; control spores showed 31% prosilition after 160 min and 83% after 220 min, while after 195 min no prosilition was observed in the presence of azide. Azide was washed away after 210 min, and no prosilition was observed after 255 min, but 72% of the cells had done so after 315 min. This indicates a rebound effect of the cells after withdrawal of azide. When spore prosilition was blocked by azide, ESR spectra showed only the first decrease in cytoplasmic viscosity. The reduced apparent viscosity of approximately 11 to 12 cP was maintained during the entire period as long as azide was in the medium, whereas spores without azide successfully underwent prosilition and had a cytoplasmic viscosity of approximately 2 cP at 175 min after the start of heat activation (Fig. 8). When azide was washed out, the cytoplasmic viscosity decreased sharply after approximately 50 min, coincident with prosilition. The parameter of anisotropic motion, h_0/h_{+1}, also decreased with prosilition (Fig. 8, inset).

However, other processes occurring during germination were not blocked. A distinct initial lowering of the optical density of the ascospore suspension was noticed in the presence of azide at the same time as in its absence (Fig. 9A). Thereafter the optical density of the control cells continued to decrease at a low rate, but that of the azide-treated cells remained constant. Trehalose degradation and the efflux of the degradation product of trehalose, glucose, occurred within the same time frame for both control cells and azide-treated cells

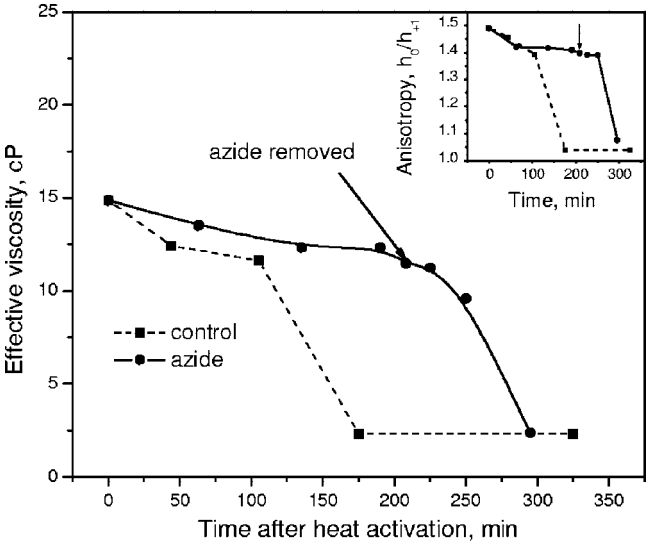

FIG. 8. Azide blocks prosilition. Shown are changes in effective cytoplasmic viscosity in germinating *T. macrosporus* ascospores in the presence or absence of 5 mM sodium azide. The first drop in viscosity did not depend on the presence of the azide. The final drop in viscosity was observed only after the azide was washed out. The inset shows the parameter of anisotropic motion.

(Fig. 9B) (13). Remarkably, these processes took place without notable oxygen consumption (Fig. 9C), while oxygen consumption increased after prosilition in the controls.

The above data suggest that the first decrease in cytoplasmic viscosity coincides with degradation of trehalose and leakage of glucose, while the second and major decrease in cytoplasmic viscosity occurs during and after prosilition. This means that the high concentration of trehalose is not the main factor determining the high effective viscosity and high level of anisotropic motion.

Conidia of *P. roqueforti* and *P. crustosum* exhibit different cytoplasmic parameters that change gradually during germination. To relate the high viscosity and degree of anisotropy observed in ascospores to their extreme longevity and resistance, we conducted a comparative study with conidia from *P. roqueforti* and *P. crustosum*. Conidia are an asexual type of spores that are less resistant to stress than ascospores and lack constitutive dormancy (a block in germination that is not taken away by the mere addition of nutrients). The PDT spectrum from conidial spores was rather complex (Fig. 10A). There was superposition of at least three spectra with different characteristics. The narrow lines, obviously, represent the PDT spectrum from the aqueous fluid phase of the cytoplasm, because the splitting a_{iso} of 16.1 G was the same as that of the spectrum of PDT in water (16.1 G; Fig. 1A), and there was no sign of broadening by ferricyanide. In addition, there was a superimposed singlet that was not observed in ascospores. The singlet did not belong to PDT molecules, as it also was observed in nonlabeled conidia (Fig. 10A, inset). Probably, this singlet originates from the green melanin-like pigment present in the spore cell wall (52). The calculated g values for the signal from nonlabeled green spores were 2.00407 (with diphenylpicrylhydrazyl as a standard) and 2.00415 (with Bruker strong pitch as a standard). These two values are within the range of the g

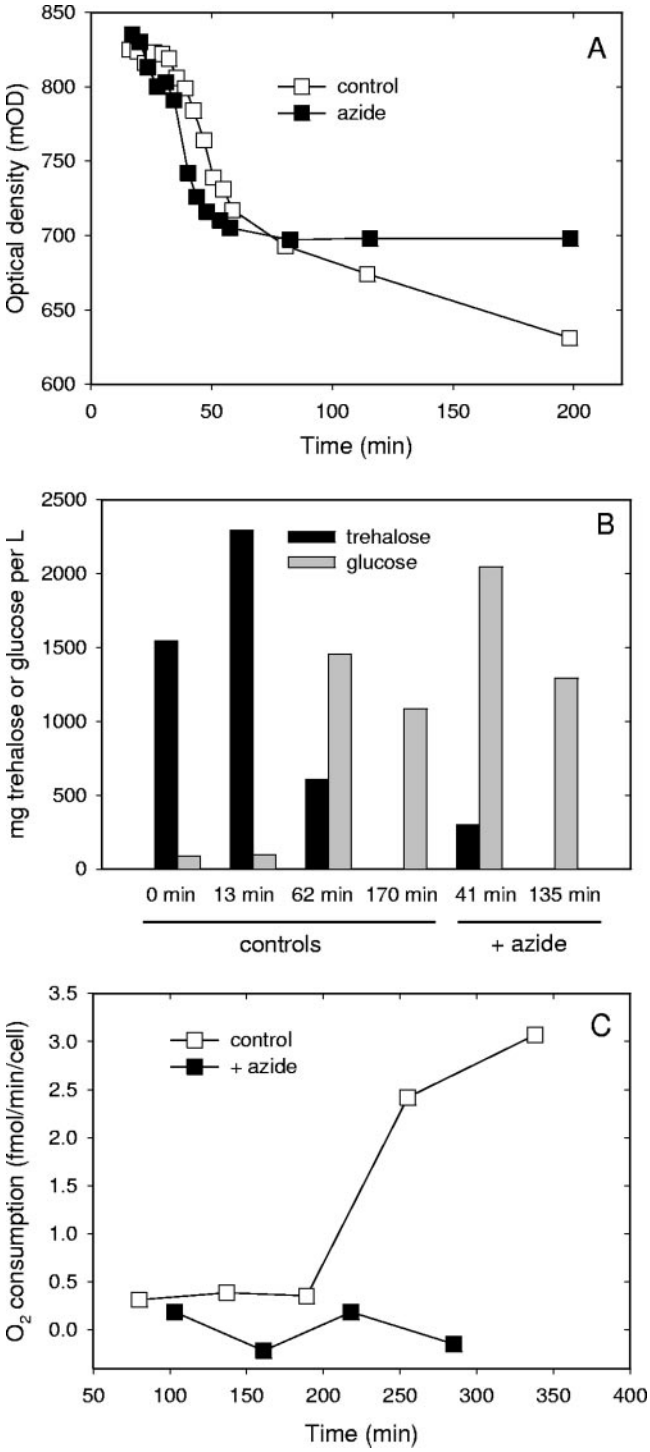

FIG. 9. Physiological phenomena during azide treatment of ascospores. Shown is the effect of 5 mM azide on the germination process of *T. macrosporus* ascospores. (A) Decrease in optical density of an ascospore suspension at 660 nm during early germination. (B) Amount of trehalose inside the spores of a fixed number of activated germinating cells. The gray bars show the total amount of glucose including glucose released by the spores and glucose present inside the spores. This is a measure of trehalose degradation. (C) Oxygen consumption during germination.

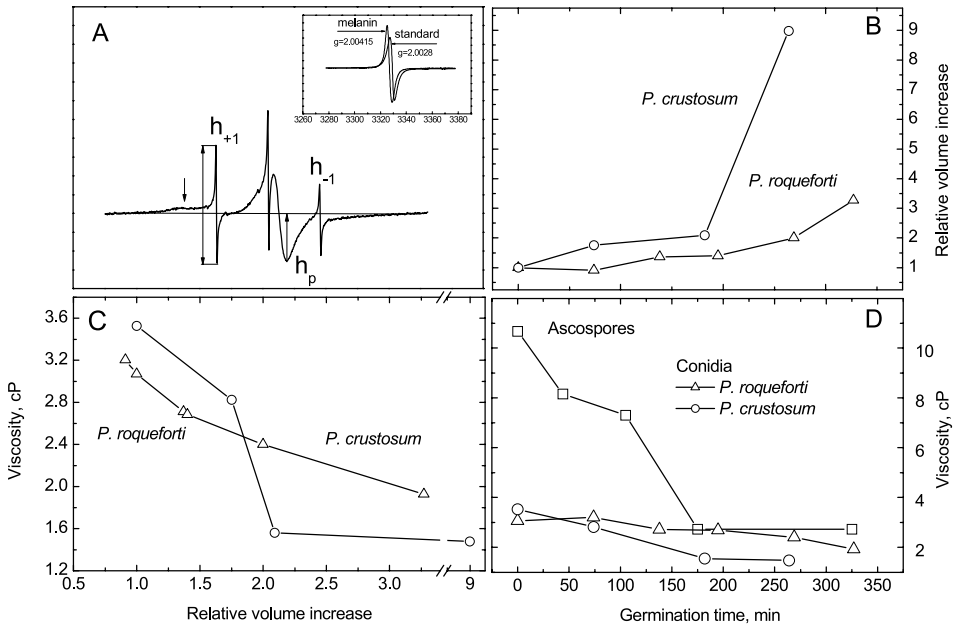

FIG. 10. ESR spectra of conidia. Data are derived from ESR spectra of PDT in conidia of *P. crustosum* and *P. roqueforti.* (A) Example of a PDT spectrum from conidial spores of *P. crustosum* showing a singlet (height = h_p) that probably originates from pigments in the cell wall (see also inset, which also shows the relative position of the signal from the standard Bruker strong pitch). (B) Using h_p as a reference for the number of cells and h_{+1} as a reference for the intracellular volume where PDT resides, the change in cellular volume during germination could be plotted. (C) Correlation between cytoplasmic viscosity and cellular volume in germinating conidia. (D) Comparison of changes in effective viscosity during germination of conidia and ascospores, using an adapted equation.

factor for melanins (2.003 to 2.0047) (4, 9, 45). The shape of the signal corresponds to that described for melanins—it was slightly asymmetric without hyperfine structure.

The third signal had an outermost splitting characteristic of immobile nitroxides (arrow in Fig. 10A). This spectral component will be ignored as it is difficult to resolve it from other components. The presence of the singlet in the spectra from conidial spores has an advantage. The amplitude of the pigment signal, h_p (Fig. 10A), is proportional to the number of cells in the sample, assuming that the pigment is stable within the 325 min of incubation (5). Normalization of the spectral lines to the height of the pigment peak h_p in the same spectrum enables the cytoplasmic volume of one cell to be estimated, as follows. The estimation is based on the fact that the narrow component of the ESR spectrum originates from PDT molecules in the aqueous phase that are inaccessible for ferricyanide ions, i.e., the total cytoplasmic volume of all cells. Because PDT molecules are equally distributed within the sample, their number is proportional to the volume. The number of PDT molecules is proportional to the area under the absorption peak. Because ESR spectra are first derivatives of absorption spectra, quantification of the number of paramagnetic molecules needs double integration to obtain the area under the absorption peaks. However, since only well-resolved spectra can be treated that way, we turned to an approximation method for integrated intensity using the only well-resolved low-field line, h_{+1}. The integrated intensity was thus calculated as $h_{+1} \times (\Delta W_{+1}{}^2)$, where ΔW_{+1} is the peak-to-peak width of the h_{+1} line (34). When divided by h_p, values were obtained that are proportional to the cytoplasmic volume of one cell. Figure 10B shows the relative volume increase with time of germination.

The presence of the singlet poses problems with further spectral analysis, because it was impossible to obtain the shape of the cytoplasmic component by subtraction of the singlet, as was done with ascospores (cf. Fig. 1B and C). Because the central line of the cytoplasmic component cannot be resolved, its height cannot be used to calculate rotational correlation time and related viscosity. However, low-field and high-field components are well resolved. In such a case there is another way to calculate rotational correlation time (28): $\tau_R = 6.5 \times 10^{-10}\ \Delta W_{-1}(\sqrt{h_{+1}/h_{-1}} - 1)$ (s), based on the heights of the low-field and high-field lines alone. This equation gives correlation times that are slightly different from those calculated with the height of the central line as indicated in Materials and Methods. To be able to compare correlation times and related apparent viscosities for conidia with those for ascospores, we recalculated these parameters for germinated ascospores in the experiment with azide (Fig. 8) in the same way as for conidial spores. Figure 10D shows the changes in cytoplasmic viscosity with time of germination for both conidial spores of *P. crustosum* and *P. roqueforti* and ascospores of *T. macrosporus*. The calculated viscosity for the conidial spores was much lower than that for the ascospores (<3.5 cP versus 10.7 cP) and decreased gradually during germination. Unfortunately, the presence of the pigment signal (singlet) did not allow for determination of the anisotropic motion parameter as was done for the ascospores.

Figure 10C shows the plot of the cytoplasmic viscosities from Fig. 10D against the relative cellular volumes depicted in Fig. 10B for the germinating conidia of both *Penicillium* species. Because the two parameters were derived from the same spectrum, the correlation between them can be plotted with great precision. It appears that viscosity inversely depended on cell

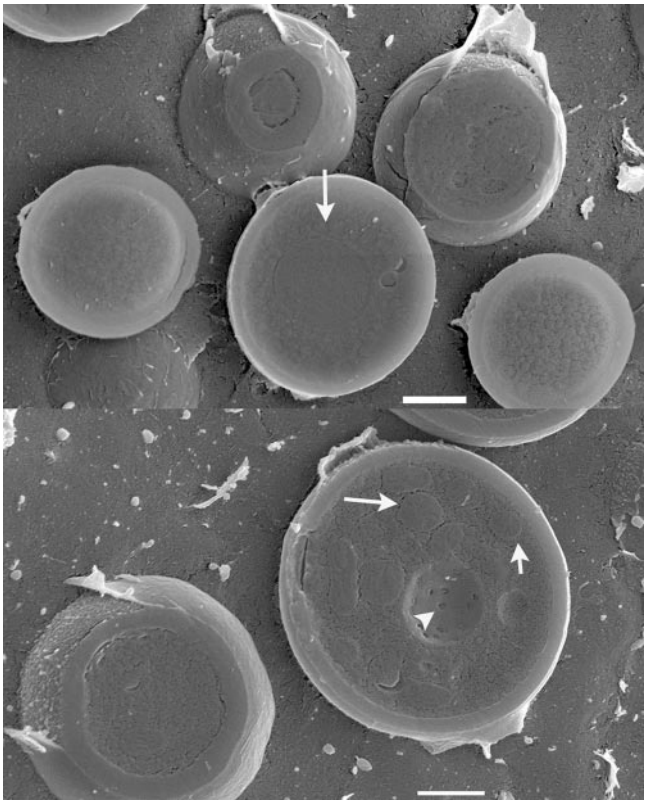

FIG. 11. Conidia of *Penicillium* species. Shown are LTSEM micrographs of etched, cryoplaned conidia of *Penicillium crustosum* (A) and *P. roqueforti* (B) directly after harvesting. These spores show the outlines of organelles (arrows). In the nucleus of *P. roqueforti* nuclear pores are visible. Bars, 1 μm.

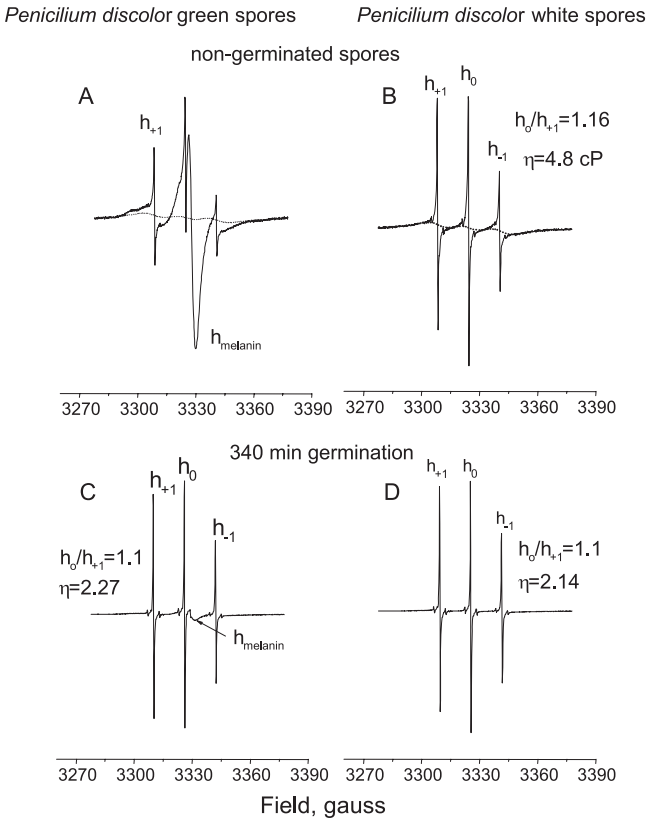

FIG. 12. Spectra from conidia from *P. discolor* and a natural mutant from this strain that forms only white conidia. (A and B) ESR spectra from ungerminated green (A) and white (B) conidia with a calculation of anisotropy and viscosity according to the methods used for ascospores. (C and D) Green (C) and white (D) conidia after 340 min of germination together with calculated values for anisotropy and viscosity.

size. This agrees with the gradual increase in size of the spores before a germ tube is formed, as will be outlined below.

Cryoplaned LTSEM images of these spores show internal cell features directly after harvesting (Fig. 11), which is consistent with the ESR observations. This indicates that the asexual, airborne conidial structures are characterized by a low effective viscosity, whereas the long-term surviving sexual ascospores are characterized by a high effective viscosity.

Natural mutants with white conidia show no melanin signal and enable the calculation of the anisotropy inside the spores. In order to compare the measurements on conidia to those on ascospores, we used a natural mutant of the *P. discolor* strain CBS 611.92 that had white conidia and compared it to the green parent strain during germination. The strains were compared by β-tubulin sequencing and metabolite pattern analysis (M. R. van Leeuwen, unpublished results) and were found to be identical. Both strains produced numerous conidia which were inoculated, and ESR spectra were recorded. Figure 12A shows that the ESR spectrum of green conidia contains a superposition of three different spectra as observed in the case of *P. crustosum* and *P. roqueforti* containing the singlet originating from melanin with the same g factor. Nonlabeled green spores did show the singlet signal (as in Fig. 10A, inset), but nonlabeled white spores did not have any ESR signal (not shown). This observation together with the value of the g factor for the singlet and the shape of the singlet (9) indicates that the endogenous ESR signal in green spores originates from free radicals trapped within the matrix of the melanin.

The ESR spectrum of white conidia is shown in Fig. 12B, and the initial viscosity (4.8 cP) and anisotropy (1.16) could be calculated according to the same method as was used for the ascospores (see Materials and Methods). In Fig. 12C and D, the spectra of green and white conidia were depicted after 340 min of germination. Microscopically, the two types of spores had been markedly swollen to similar extents. With the green spores the ESR parameters could be calculated reasonably accurately because of the lowered impact of the singlet on the spectrum. In Fig. 12D the singlet was absent and the narrow signal very dominating. The calculated anisotropies for the two spectra (Fig. 12C and D) had the same value of 1.1, and the calculated viscosities, based on the h_0/h_{+1} ratio, were 2.27 cP for green germinated spores and 2.14 cP for white germinated spores. These observations confirmed that the viscosity calculated by the alternative method, described above for conidia, was realistic. Further, the anisotropy inside conidia could be calculated as in ascospores.

The volume of ascospores does not change during gross changes in cytoplasmic organization. The presence of a stable natural radical (green pigment) in the conidia enabled the relative volume increase with germination time to be calcu-

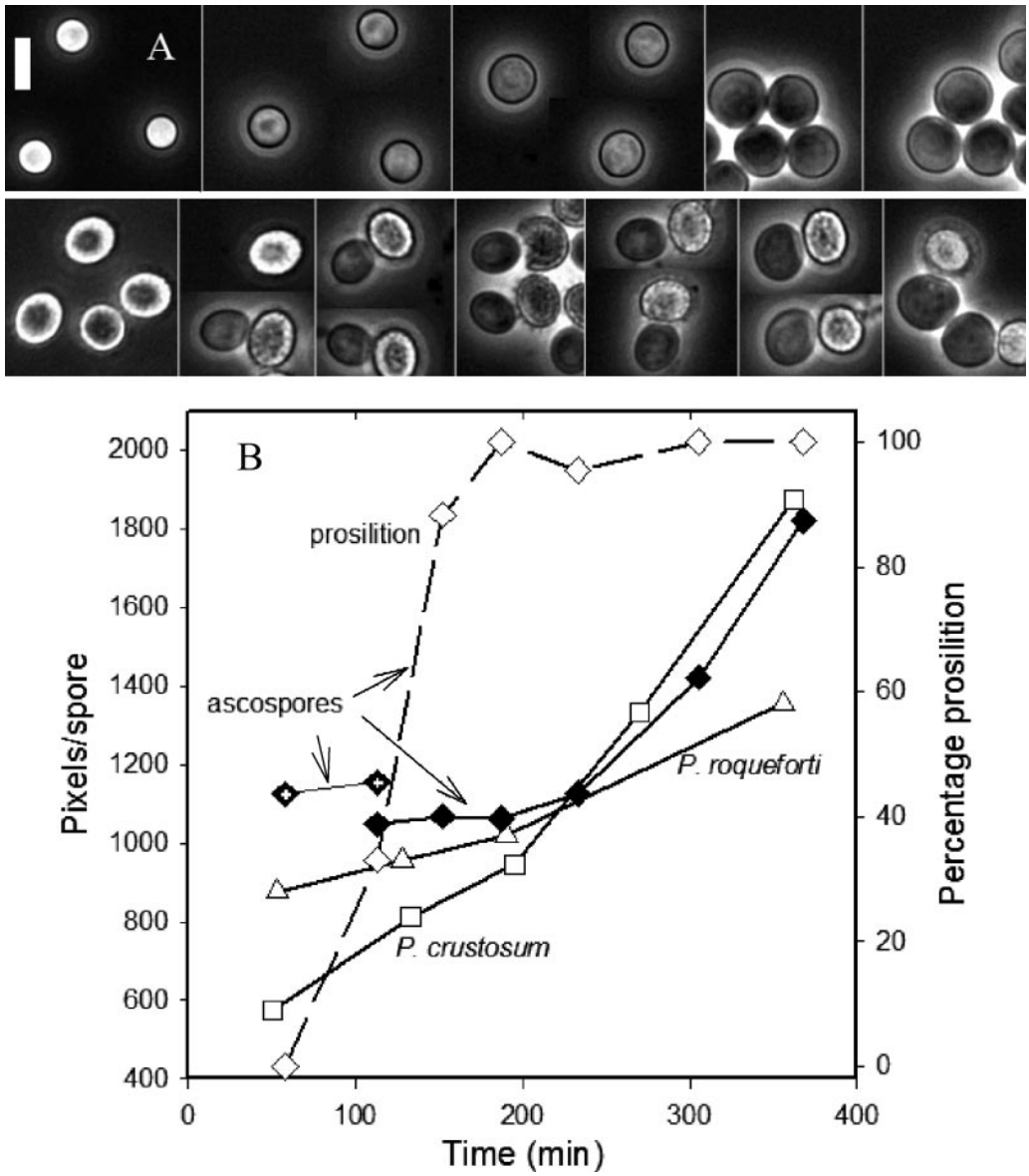

FIG. 13. Cell size of ascospores and conidia during germination. (A) Micrographs of *P. crustosum* conidia, inspected during five stages of development (from left to right) after 50, 133, 195, 270, and 362 min of incubation, respectively (top panel), and micrographs of *T. macrosporus* ascospores, viewed during seven stages of development (left to right; after 58, 113, 152, 187, 233, 305, and 368 min of incubation, respectively [bottom panel]). Bar, 5 μm. (B) Surface area increase of conidia (*P. crustosum* [open squares] and *P. roqueforti* [open triangles]) and *T. macrosporus* ascospores during germination (closed diamonds, with a cross for the nonejected cells). The open diamonds show the percentage of ascospores that have undergone prosilition at each stage.

lated from the ESR spectral parameters (Fig. 10B). On the basis of the plot of viscosity versus volume increase (Fig. 10C), it was argued that in conidia the decrease in viscosity could be ascribed to volume increase. To examine whether this is also the case for the ascospores, a morphometric analysis was conducted with both types of spores. Figure 13 shows the gradual surface area increase for the conidia, which supports the gradual volume increase that emerged from ESR work in Fig. 10. In contrast, the ascospores showed no apparent surface area increase during early germination until after 230 min, while the majority of the cells had undergone prosilition after 150 min. Initially only ascospores with the thick outer cell wall were measured, and later the ejected cells, which gave slightly smaller surface areas, were measured. From the LTSEM micrographs it became clear that on prosilition the entire protoplast is ejected. Thus, the decrease in viscosity and anisotropy with ascospore prosilition as shown in Fig. 3 is not caused by volume increase.

DISCUSSION

Conidia and ascospores: two types of fungal survival cells. In this study, spin probe ESR combined with LTSEM has provided us with novel insights into the biology of fungal

spores. The observations show that the mechanisms of cytoplasm conservation and germination in the highly resistant ascospores of *T. macrosporus* are different from those in the less-stress-resistant conidia. Very high effective cytoplasmic viscosity and levels of anisotropic motion were found for dormant *T. macrosporus* ascospores. Also, the time lag between dormancy and prosilition was characterized by such high values, but a dramatic and fast decrease was noticed with prosilition. By comparison, conidia of different *Penicillium* species had much lower cytoplasmic viscosity that gradually decreased with isotropic growth (swelling) during germination. These observations can be linked to the lifestyles of the different types of survival cells. Ascospores of *T. macrosporus* belong to a type of spores that are formed in (closed) fruiting bodies and are constitutively dormant and highly stress resistant. They are designed to survive for long periods and literally "wait" for suitable growth conditions. Their cytoplasm and membranes have to be protected for a prolonged time, and dormancy is often profound (see reference 40). Conidia are formed on conidiophores that lift these spores into the air for release and transport to novel nutrient-rich locations where they have to germinate rapidly in response to proper nutrient conditions. They need protection against drought but have reduced longevity of survival and dormancy compared to ascospores (18).

Ascospores possess a unique, very crowded cytoplasm with high anisotropy. We used the deuterated form of TEMPONE as the molecule for probing cytoplasmic surroundings. Although this spin probe is considered a small, noninteracting molecule suitable to study fluid-phase viscosity of the cytoplasm, values (2 to 6 cP) obtained by this approach are usually higher (38, 48) than those (1.1 to 1.5 cP) obtained with fluorescent probes. This was particularly the case when the bound fluorescent molecules were excluded from the calculations (20, 43, 44, 50). Possible interaction of spin probe molecules with cytoplasmic components may thus contribute to the slightly higher cytoplasmic viscosities found with the spin probe method. Our values for cytoplasmic viscosity obtained for ascospores that had undergone prosilition (around 2 cP) and for conidial spores (from 4.8 to 1.7 cP during 4.5 h of germination) agree well with published ESR data on cytoplasmic viscosity (35, 39, 48). However, the high viscosity values obtained for dormant ascospores (>10 cP) are unique. They are comparable only with old ESR-derived data for *Escherichia coli* and anaerobic yeast cells (25) and with recent data for stress-resistant bacterial spores (Y. de Vries, unpublished data). The viscosity data for *E. coli* and anaerobic yeast cells (25) are probably overestimations due to the osmotic effect brought about by the excessive amount of $NiCl_2$ used to broaden the extracellular probe signal. These authors explained the high in vivo viscosity as the result of the probe's behavior in extensive internal membrane structures and not of high osmolality, because a 1.6 M sucrose solution gave a correlation time corresponding to the relatively low viscosity of 1.5 cP.

The ESR spectra had another important characteristic: the anisotropy parameter h_0/h_{+1}, which was high (1.4) in dormant ascospores (Fig. 3, inset). This high ratio can be interpreted as the result of the preferential rotation of the spin probe molecules about the molecular *y* axis. In our opinion, the $h_0/h_{+1} \gg 1$ obtained for dormant ascospores is related to some ordering of PDT molecules. Thus, the high cytoplasmic viscosity together with the high values of h_0/h_{+1} might be caused by ordering of spin probe molecules in the vicinity of macromolecules in a highly crowded cytoplasm.

With prosilition, the proportion of ordered spin probe molecules decreased ($h_0/h_{+1} = 1.08$; Fig. 3, inset). Because there was no increase in volume (Fig. 13) that could have led to decreases in anisotropic motion and effective viscosity, it is likely that some other property of the cytoplasm had changed. Also, it is unlikely that trehalose is involved, because it had degraded prior to prosilition (Fig. 9B) directly followed by the efflux of the degradation product, glucose, into the surrounding medium (see also reference 13). The loss of these compounds was responsible for only part of the reduction in fluid-phase viscosity inside the cell (Fig. 3). The still-high effective viscosity prior to prosilition, even in the absence of trehalose, suggests that the spore cytoplasm must be highly ordered structurally. The nature of this high viscosity is an enigma. We have observed an increase in mannitol related to the ascospores after trehalose degradation, but whether this is enough to account for the observed phenomenon is unknown (J. Dijksterhuis, unpublished results). One can speculate if heat shock proteins play an important role in cooperation with compatible solutes in yeasts (17), but these are rarely studied in fungal survival structures. Recently, the genome of the filamentous fungus *Aspergillus fumigatus* was sequenced (41), and 323 genes showed higher expression at 48°C than at 37°C. The most strongly upregulated genes included three proteins related to compatible solute synthesis and degradation and nine heat shock proteins.

This could mean that the high effective cytoplasmic viscosity obtained in our study for ascospores that had not undergone prosilition does not relate to the real viscosity of the fluid phase but is associated with a high proportion of ordered PDT molecules in the vicinity of macrostructures. It is interesting that the occurrence of a glassy cytoplasm in LTSEM images of ascospores coincided with a high effective viscosity as derived from ESR spectra. Apparently, a high effective cytoplasmic viscosity prevents fast ice nucleation when the cells are plunged into liquid propane for LTSEM processing. Conversely, low effective viscosity goes together with faster ice nucleation, as observed in conidia throughout the swelling period and in ascospores that have undergone prosilition.

Sudden exposition of the internal spore is an important mechanism for renormalization to the vegetative stage in long-term-dormant ascospores. Prosilition, a process during which the thick outer cell wall breaks and the complete inner spore is released in a very quick process (seconds), is a prerequisite for renormalization of the cytoplasm towards a vegetative condition in *T. macrosporus*. Sudden opening of an outer cell wall also has been observed in ascospores of *Hypoxylon fragiforme* (7, 8), and a germinal slit has been observed in the cell wall of *Daldinia concentrica* (1, 2). Recently, we observed prosilition in the case of four other *Talaromyces* species and found an indication that also the heat-resistant ascospores of *Neosartorya fischeri* exhibit rupture of the outer cell wall during early germination (J. Dijksterhuis, unpublished results). Combined, these observations suggest that rupture of an outer thick cell wall and the associated exposure of the inner spore, which possesses a much thinner cell wall, to the environment are general mechanisms in ascospore germination and prerequisites for

renormalization of the spore for further vegetative growth. Prevention of these processes, e.g., by azide, keeps the cells in the "dense" state, but on release of the inhibition, the internal viscosity decreases in conjunction with ejection of the protoplast. As argued before, the latter event is associated with a near-constant volume of the spores, indicating that the cytoplasmic structure undergoes considerable changes during these stages of germination.

After prosilition, oxygen consumption strongly increased and swelling of the vegetative cell occurred (Fig. 9C and 13B) (see also reference 13), followed by the formation of a germ tube. The low level of biosynthetic activity during early ascospore germination is corroborated by the work of Plesofsky-Vig et al. (46) and Hill et al. (22) while working on *Neurospora tetrasperma*. These authors observed low protein and RNA synthesis during early germination for a period of hours.

Freshly harvested conidia that lack constitutive dormancy and have less resistance to stress than ascospores were characterized by low effective viscosity (Fig. 10D) and anisotropy (Fig. 12B). The latter could be calculated only in a natural mutant of *P. discolor*, while green conidia exhibit a disturbed spectrum most probably due to the presence of melanin. LT-SEM images revealed cell organelles in ungerminated conidial spores (Fig. 11), confirming the lower cytoplasmic viscosity.

After incubation of the conidia in growth medium the cell diameter gradually enlarges by isotropic growth ("swelling") followed by the appearance of a germ tube after 7 or more h (polarized growth) (see for instance reference 36). The slow decrease in effective viscosity of conidia is most likely linked with the gradual increase in cytoplasmic volume as derived from ESR spectral data (Fig. 10) and confirmed by the light microscopy analysis (Fig. 13). In contrast, the sudden drop in viscosity of ascospores during prosilition, associated with the return to vegetative growth, is not linked with volume changes but rather reflects sudden changes in the structural organization of the cytoplasm.

ACKNOWLEDGMENTS

We thank Mark Sanders for trehalose and glucose determinations and Kenneth van Driel for help during several experiments. We are indebted to Adriaan van Aelst for advice and help during cryoplaning sessions and Douwe Molenaar for help with oxygen consumption measurements.

REFERENCES

1. **Beckett, A.** 1976. Ultrastructural studies on exogenously dormant ascospores of *Daldinia concentrica*. Can. J. Bot. **54:**689–697.
2. **Beckett, A.** 1976. Ultrastructural studies on germinating ascospores of *Daldinia concentrica*. Can. J. Bot. **54:**698–705.
3. **Blacklow, S. C., R. T. Raines, W. A. Lim, P. D. Zamore, and J. R. Knowles.** 1988. Triosephosphate isomerase catalysis is diffusion controlled. Biochemistry **27:**1158–1167.
4. **Blois, M. S., A. B. Zahlan, and J. E. Maling.** 1964. Electron spin resonance studies of melanin. Biophys. J. **4:**471–490.
5. **Butler, M. J., and A. W. Day.** 1998. Fungal melanins: a review. Can. J. Microbiol. **44:**1115–1136.
6. **Carlisle, M. J., S. C. Watkinson, and G. W. Gooday.** 2001. The fungi, p. 185–243. Academic Press, London, United Kingdom.
7. **Chapela, I. H., O. Petrini, and L. E. Petrini.** 1990. Unusual ascospore germination in *Hypoxylon fragiformi:* first steps in the establishment of an endophytic symbiosis. Can. J. Bot. **68:**2571–2575.
8. **Chapela, I. H., O. Petrini, and L. Bielser.** 1993. The physiology of ascospore eclosion in *Hypoxylon fragiformi:* mechanisms in the early recognition and establishment of an endophytic symbiosis. Mycol. Res. **97:**157–162.
9. **Chauffer, L., J. Windle, and M. Friedman.** 1975. Electron spin resonance study of melanin treated with reducing agents. Biophys. J. **15:**565–572.
10. **Conner, D. R., L. R. Beuchat, and C. J. Chang.** 1987. Age-related changes in ultrastructure and chemical composition associated with changes in heat resistance of *Neosartorya fischeri* ascospores. Trans. Br. Mycol. Soc. **89:**539–550.
11. **Creighton, T. E.** 1997. Protein folding: does diffusion determine the folding rate? Curr. Biol. **7:**R380–R383.
12. **Demchenko, A. P., O. I. Rusyn, and E. A. Saburova.** 1989. Kinetics of the lactate dehydrogenase reaction in high-viscosity media. Biochim. Biophys. Acta **998:**196–203.
13. **Dijksterhuis, J., K. G. A. van Driel, M. G. Sanders, D. Molenaar, J. A. M. P. Houbraken, R. A. Samson, and E. P. W. Kets.** 2002. Trehalose degradation and glucose efflux precede cell ejection during germination of heat-resistant ascospores of *Talaromyces macrosporus*. Arch. Microbiol. **178:**1–7.
14. **Dijksterhuis, J., and P. G. M. Teunissen.** 2004. High-pressure treatments can induce germination of dormant ascospores of *Talaromyces macrosporus*. J. Appl. Microbiol. **96:**162–169.
15. **Dijksterhuis, J., and R. A. Samson.** 2006. Activation of stress-resistant ascospores by novel food preservation techniques. Adv. Exp. Med. Biolog. **571:**247–260.
16. **Dix, J. A., and A. S. Verkman.** 1990. Mapping of fluorescence anisotropy in single cells by ratio imaging. Application to cytoplasmic viscosity. Biophys. J. **57:**231–240.
17. **Elliot, B., R. S. Haltiwanger, and B. Futcher.** 1996. Synergy between trehalose and Hsp104 for thermotolerance. Genetics **144:**923–933.
18. **Fillinger, S., M.-K. Chaveroce, P. van Dijck, R. P. de Vries, G. Ruijter, J. Thevelein, and C. d'Enfert.** 2001. Trehalose is required for the acquisition of tolerance to a variety of stresses in the filamentous fungus *Aspergillus nidulans*. Microbiology **147:**1851–1862.
19. **Frisvad, J. C., O. Filtenborg, R. A. Samson, and A. C. Stolk.** 1990. Chemotaxonomy of the genus *Talaromyces*. Antonie Leeuwenhoek **57:**179–189.
20. **Fushimi, K., and A. S. Verkman.** 1991. Low viscosity in the aqueous domain of cell cytoplasm measured by picosecond polarization microfluorimetry. J. Cell Biol. **112:**719–725.
21. **Golovina, E. A., and F. A. Hoekstra.** 2003. Acquisition of desiccation tolerance in developing wheat embryos correlates with appearance of a fluid phase in membranes. Plant Cell Environ. **26:**1815–1826.
22. **Hill, E. P., N. Plesofsky-Vig, A. Paulson, and R. Brambl.** 1992. Respiration and gene expression in germinating ascospores of *Neurospora tetrasperma*. FEMS Microbiol. Lett. **69:**111–115.
23. **Jacob, M., and F. X. Schmid.** 1999. Protein folding as a diffusional process. Biochemistry **38:**13773–13779.
24. **Keith, A., G. Bulfield, and W. Snipes.** 1970. Spin-labeled *Neurospora* mitochondria. Biophys. J. **10:**618–629.
25. **Keith, A. D., and W. Snipes.** 1974. Viscosity of cellular protoplasm. Science **183:**666–668.
26. **Keith, A. D., W. Snipes, and D. Chapman.** 1977. Spin label studies on the aqueous regions of phospholipid bilayers. Biochemistry **16:**634–641.
27. **Klimov, D. K., and D. Thirumalai.** 1997. Viscosity dependence of the folding rates of proteins. Phys. Rev. Lett. **79:**317–320.
28. **Kuznetsov, A. N., A. M. Wasserman, A. U. Volkov, and N. N. Korst.** 1971. Determination of rotational correlation time of nitric oxide radicals in a viscous medium. Chem. Phys. Lett. **12:**103–106.
29. **Lepock, J. R., K. H. Chang, S. D. Campbell, and J. Kruuv.** 1983. Rotational diffusion of tempone in the cytoplasm of Chinese hamster lung cells. Biophys. J. **44:**405–412.
30. **Luby-Phelps, K., P. E. Castle, D. L. Taylor, and F. Lanni.** 1987. Hindered diffusion of inert tracer particles in the cytoplasm of mouse 3T3 cells. Proc. Natl. Acad. Sci. USA **84:**4910–4913.
31. **Luby-Phelps, K., D. L. Taylor, and F. Lanni.** 1986. Probing the structure of cytoplasm. J. Cell Biol. **102:**2015–2022.
32. **Luby-Phelps, K., F. Lanni, and D. L. Taylor.** 1988. The submicroscopic properties of cytoplasm as a determinant of cellular function. Annu. Rev. Biophys. Biophys. Chem. **17:**369–396.
33. **Luby-Phelps, K.** 1994. Physical properties of cytoplasm. Curr. Biol. **6:**3–9.
34. **Marsh, D.** 1981. Electron spin resonance: spin labels. Mol. Biol. Biochem. Biophys. **31:**51–142.
35. **Mastro, A. M., M. A. Babich, W. D. Taylor, and A. D. Keith.** 1984. Diffusion of a small molecule in the cytoplasm of mammalian cells. Proc. Natl. Acad. Sci. USA **81:**3414–3418.
36. **Momany, M.** 2002. Polarity in filamentous fungi: establishment, maintenance and new axes. Curr. Opin. Microbiol. **5:**580–585.
37. **Morse, P. D. II.** 1985. Structure-function relationships in cell membranes as revealed by spin labeling EPR, p. 195–236. *In* G. Benga (ed.), Structure and properties of cell membranes, vol. 3. CRC Press, Boca Raton, FL.
38. **Morse, P. D. II.** 1977. Use of the spin label tempamine for measuring the internal viscosity of red blood cells. Biochem. Biophys. Res. Commun. **77:**1486–1491.
39. **Morse, P. D. II, D. M. Lusczakoski, and D. A. Simpson.** 1979. Internal microviscosity of red blood cells and hemoglobin-free resealed ghosts: a spin-label study. Biochemistry **18:**5021–5029.
40. **Nagtzaam, M. P. M., and G. J. Bollen.** 1994. Long shelf life of *Talaromyces flavus* in coating material of pelleted seeds. Eur. J. Plant Pathol. **100:**279–282.

41. **Nierman, W. C., et al.** 2005. Genomic sequence of the pathogenic and allergenic filamentous fungus *Aspergillus fumigatus*. Nature **438:**1151–1156.
42. **Nijsse, J., and A. C. van Aelst.** 1999. Cryo-planing for cryoscanning electron microscopy. Scanning **21:**372–378.
43. **Periasamy, N., M. Armijo, and A. S. Verkman.** 1991. Picosecond rotation of small polar fluorophores in the cytosol of sea urchin eggs. Biochemistry **30:**11836–11841.
44. **Periasamy, N., H. P. Kao, K. Fushimi, and A. S. Verkman.** 1992. Organic osmolytes increase cytoplasmic viscosity in kidney cells. Am. J. Physiol. **263:**C901–C907.
45. **Pilawa, B., E. Buszman, A. Gondzik, S. Wilczynski, M. Zdybel, T. Witoszynska, and T. Wilczok.** 2005. Effect of pH on paramagnetic centers in *Cladosporium cladosporioides* melanin. Acta Physiol. Pol. **108(A):**147–150.
46. **Plesofsky-Vig, N., A. Paulson, E. P. Hill, L. Glaser, and R. Brambl.** 1992. Heat shock gene expression in germinating ascospores of *Neurospora tetrasperma*. FEMS Microbiol. Lett. **69:**117–122.
47. **Ruijter, G. J. G., M. Bax, H. Patel, S. J. Flitter, P. J. L. van de Vondervoort, R. P. de Vries, P. A. van Kuyk, and J. Visser.** 2003. Mannitol is required for stress tolerance in *Aspergillus niger* conidiospores. Eukaryot. Cell **2:**690–698.
48. **Schobert, B., and D. Marsh.** 1982. Spin label studies on osmotically induced changes in the aqueous cytoplasm of *Phaeodactylum tricornutum*. Biochim. Biophys. Acta **720:**87–95.
49. **Scholte, R. P. M., R. A. Samson, and J. Dijksterhuis.** 2004. Spoilage fungi in the industrial processing of food, p. 339–356. *In* R. A. Samson, E. S. Hoekstra, and J. C. Frisvad (ed.), Introduction to food- and airborne fungi, 7th ed. Centraalbureau voor Schimmelcultures, Utrecht, The Netherlands.
50. **Srivastava, A., and G. Krishnamoorthy.** 1997. Cell type and spatial location dependence of cytoplasmic viscosity measured by time-resolved fluorescence microscopy. Arch. Biochem. Biophys. **340:**159–167.
51. **Sussman, A. S., and H. O. Halvorson.** 1966. Spores: their dormancy and germination. Harper and Row, New York, NY.
52. **Youngchim, S., R. J. Hay, and A. J. Hamilton.** 2005. Melanization of *Penicillium marneffei in vitro* and *in vivo*. Microbiology **151:**291–299.